



ELSEVIER

Contents lists available at ScienceDirect

Deep-Sea Research I

journal homepage: www.elsevier.com/locate/dsri

Sinking particle flux in the sea ice zone of the Amundsen Shelf, Antarctica

Minkyoung Kim^a, Jeomshik Hwang^{a,*}, Hyung J. Kim^b, Dongseon Kim^b, Eun J. Yang^c, Hugh W. Ducklow^d, Hyoung S. La^c, Sang H. Lee^e, Jisoo Park^c, SangHoon Lee^c^a School of Earth and Environmental Sciences/Research Institute of Oceanography, Seoul National University, Seoul, South Korea^b Korea Institute of Ocean Science & Technology, Ansan, South Korea^c Korea Polar Research Institute, Incheon, South Korea^d Lamont-Doherty Earth Observatory, Columbia University, Palisades, NY, USA^e Pusan National University, Busan, South Korea

ARTICLE INFO

Article history:

Received 27 September 2014

Received in revised form

26 March 2015

Accepted 3 April 2015

Available online 16 April 2015

Keywords:

Particulate organic carbon

Particle flux

Sea ice zone

Sediment trap

Amundsen Sea

Radiocarbon

ABSTRACT

We have examined the flux, biogenic composition, and isotopic values of sinking particles collected by a time-series sediment trap deployed in the sea ice zone (SIZ) of the Amundsen Sea from January 2011 for 1 year. The major portion of the particle flux occurred during the austral summer in January and February when sea ice concentration was reduced to <60%. Biogenic components, dominated by opal (~78% of the biogenic components), accounted for over 75% of particle flux during this high-flux period. The dominant source of sinking particles shifted from diatoms to soft-tissued organisms, evidenced by high particulate organic carbon (POC) content (>30%) and a low bio-Si/POC ratio (<0.5) during the austral winter. CaCO₃ content and its contribution to total particle flux was low (~6%) throughout the study period. Aged POC likely supplied from sediment resuspension accounted for a considerable fraction only from October to December, which was evidenced by a low radiocarbon content and relatively high (30–50%) content of the non-biogenic components. When compared with POC flux inside the Amundsen Sea polynya obtained by the US Amundsen Sea Polynya International Research Expedition (ASPIRE), the POC flux integrated over the austral summer in the SIZ was virtually identical, although the maximum POC flux was approximately half that inside the Amundsen Sea polynya. This comparatively high POC flux integrated over the austral summer in the SIZ may be caused by phytoplankton blooms persisting over a longer periods and more efficient export of organic matter potentially owing to the diatom-dominant plankton community. If this observation is a general phenomenon on the Amundsen Shelf, the role of the SIZ, compared with the polynyas, need to be examined more carefully when trying to characterize the POC export in this region.

© 2015 The Authors. Published by Elsevier Ltd. This is an open access article under the CC BY-NC-ND license (<http://creativecommons.org/licenses/by-nc-nd/4.0/>).

1. Introduction

The West Antarctic, especially the Bellingshausen Sea and the Amundsen Sea, is experiencing rapid decline in sea ice cover (Stammerjohn et al., 2012). Intrusion of the warm Circumpolar Deep Water (CDW) onto the Amundsen Shelf reportedly provides the necessary heat for melting of sea ice and ice shelf (Walker et al., 2007; Wählin et al., 2010). Physical changes accompanying the decreasing sea ice are likely to affect the biogeochemistry and biology in this region. However, our understanding of the

biological carbon pump on the Amundsen Shelf is very limited because of the logistical difficulty with access (Yager et al., 2012).

Studies of the biological carbon pump of the Amundsen Sea have been based on the observations by satellites (Arrigo and van Dijken, 2003). The Amundsen Sea polynya is of particular interest because of its extremely high primary productivity during the austral summer (Arrigo and van Dijken, 2003; Arrigo et al., 2012a). Estimates of primary production based on satellite observation on the Amundsen Shelf were supported by recent *in situ* measurements (Lee et al., 2012). However, a limitation of the satellite data exists in the sense that few data are available for ice-covered regions (Arrigo et al., 2008). In addition, the process that particulate organic matter (POM) undergoes after production needs to be understood to characterize the biological pump system and the role of this region in absorption of atmospheric CO₂. Studies of

* Corresponding author.

E-mail address: jeomshik@snu.ac.kr (J. Hwang).

sinking POM flux at a depth on the Amundsen Shelf can further our understanding of carbon cycling in this region.

Compared with polynyas that have attracted attention in terms of their role in the absorption of atmospheric CO₂ because of their extremely high primary production, the role of the sea ice zone (SIZ) is not well understood. The SIZ in this research is defined as the region where sea ice concentration decreases in summer but is not ice-free, unlike polynyas (National Snow and Ice Data Center, NSIDC). In the SIZ, primary production occurs not only in water but also under sea ice (Arrigo et al., 2012b) and in sea ice (Lizotte, 2001; Thomas and Dieckmann, 2002). Thomas et al. (1998) suggested the possibility of high primary production even in areas of dense pack ice in the Bellingshausen and Amundsen Seas. Dominant plankton species of a given environment, such as *Phaeocystis antarctica* (hereafter *P. antarctica*) and diatoms, and potential shift in plankton community composition may influence the biological pump efficiency in the Southern Ocean (Arrigo et al., 1999; DiTullio et al., 2000; Smith et al., 2014). Evolution of the plankton community in the SIZ may be different from that in polynyas (Lee et al., 2012; Alderkamp et al., 2012; Smith et al., 2014).

A multidisciplinary research project was launched by the Korea Polar Research Institute (KOPRI) to examine the biological carbon pump currently operating in the Amundsen Sea. As a part of this project, we designed a time-series sediment trap study to examine POM export and its major controlling factors in the SIZ and inside the Amundsen Sea polynya. Unfortunately, due to a technical failure, no samples were obtained from the sediment trap deployed in the central polynya. We describe the detailed results of the sinking particle samples in the SIZ only. Then we compare our results with those obtained from sinking particle samples collected at a 350 m depth inside the polynya by the US Amundsen Sea Polynya International Research Expedition (ASPIRE, (Ducklow et al., 2015)).

2. Methods

A bottom-tethered hydrographic mooring with a sediment trap was deployed on the 530 m isobath (72.40 °S, 117.72 °W) on the western side of a glacier-carved trough (Dotson Trough) connecting the shelf break and the Dotson and Getz Ice Shelves (Fig. 1). Current meters (RCM-11) were attached at 253 m and 409 m depths on the same mooring (detailed design of the mooring line is available in Ha et al. (2014)). Less saline (salinity < 34.2) and colder (potential temperature < -1 °C) water occupied the upper layer shallower than ~400 m above more saline and warmer water at the mooring site (Ha et al., 2014). Northward flow was observed more frequently in this upper layer (Ha et al., 2014). The vertical gradient in potential temperature and salinity in the upper water column above ~400 m was much smaller than that below this depth to the bottom, where a southward inflow of warm CDW was prevalent (Ha et al., 2014). The current speed measured at 409 m for a year was 5 cm s⁻¹ on average. The current speed was higher in January and February (7.5 ± 3.3 cm s⁻¹ on average) than in the other months (4.4 ± 2.4 cm s⁻¹). The pressure registered by a MicroCAT (Sea-Bird Electronics) moored at 409 m fluctuated daily with an amplitude of < 1.7 dbar due to the tide and did not show any out-of-phase signal caused by tilting of the mooring line.

In this study, we used daily sea ice concentration data derived from SSMIS F-17 microwave remote sensor, retrieved from the University of Bremen (<http://www.iup.uni-bremen.de:8084/ssmis/>). The data were processed using a Bootstrap algorithm with 25 km² grid resolution. The sea ice concentration at the mooring site varied seasonally with high interannual variability. For example, the minimum sea ice concentration was 0, 37, and 56% in January and February 2010, January 2011, and March 2012, respectively. A reduced sea ice concentration below ~70% was

observed from late December 2009 to late March 2010, from December 2010 to late February 2011, and from late January to early March 2012.

Sinking particle samples were collected by deploying a time-series sediment trap (McLane, conical type, aperture diameter=80 cm, and height/diameter=2.5) at 400 m from January 2011 to January 2012 in the SIZ of the Amundsen Shelf (K1 trap). The sample cup opening interval was set between 9 and 31 days depending on the expected particle flux at the study site (Table 1). Sampling bottles were filled with filtered seawater (45 mm GF/F filter; 0.7 μm nominal pore size), collected at a 400 m depth at the sediment trap mooring site, containing 5% formalin solution buffered with sodium borate. Recovered particle samples were stored in the refrigerator at 4 °C until further treatment. Recovered samples were not fortified with fresh formalin. The pH of the solution in the sampling bottles was not determined upon recovery. The US ASPIRE sediment trap (Technicap, cylindrical type) was deployed at a 350 m depth inside the polynya (73.82°S, 113.07°W; 785 m water depth (Ducklow et al., 2015)).

Any conspicuous swimmers were removed by tweezers before dividing the samples into 10 equal aliquots using a wet-sample divider (McLane Research Laboratories). Seven aliquots of each sample were combined, rinsed with ultrapure (Millipore) water, and freeze-dried for total mass and biogenic component analyses. Total dry mass was determined gravimetrically. Details of the analyses for the biogenic components of the particles have been published elsewhere (Kim et al., 2012). Briefly, total carbon content was determined using an elemental analyzer (Carlo-Erba 1110 CNS EA) on ~10 mg samples with an uncertainty of 2% relative standard deviation (RSD). Particulate inorganic carbon (PIC) content was determined by coulometric titration (UIC Coulometrics carbon analyzer) on ~15 mg samples with an RSD of 0.2% based on repeated analyses of a CaCO₃ standard. Organic carbon content was estimated as the difference between the total and particulate inorganic carbon contents. Organic matter content was estimated by multiplying the particulate organic carbon (POC) content by 2.5 (Thunell, 1998). CaCO₃ content was estimated by multiplying the PIC content by 8.33. Opal content was estimated by multiplying the biogenic Si (Bio-Si) content by 2.4, determined by a sequential dissolution method using 0.5 N NaOH solution at 85 °C (DeMaster, 1981; Mortlock and Froelich, 1989). The precision based on 10 duplicate analyses was 15% (RSD). The difference between the total amount and the sum of the three biogenic components was defined as non-biogenic components. The error associated with this estimation was 52 ± 41% (RSD; see Table 1).

One aliquot of each sample was used for isotopic analyses. The effect of formalin as a preservative on radiocarbon analysis was determined to be insignificant in a previous study (Otosaka et al., 2008). Each sample with a sizeable amount upon visual inspection (samples #1–#9) was filtered on a pre-cleaned Nuclepore filter (Whatman membrane, 47 mm, 1.0 μm pore size) rinsing three times with ultrapure (Millipore) water. Samples were dried at 45 °C in an oven, and particles were recovered from the filter pads. Each sample was ground using a mortar and pestle, then ~20 mg dry sample was weighed in a silver cup and fumigated with concentrated HCl in a desiccator for ~20 h (Hedges and Stern, 1984; Komada et al., 2008). Small samples were filtered on pre-combusted 47 mm GF/F filters. These particle samples were not separated from the filter pads. Each pair of samples (#13 and #14, #15 and #16, #17 and #18, and #20 and #21) was combined together to obtain enough carbon for radiocarbon measurements. HCl-fumed samples were then placed on a hot plate at ~45 °C for 4 h to remove HCl vapor. The sample cup was placed in a quartz tube with CuO. The sample tube was evacuated on a vacuum line and flame-sealed, then combusted at 850 °C for 4 h. Particle samples on GF/F filters were treated in the same way except that silver wire was added instead of a silver cup.

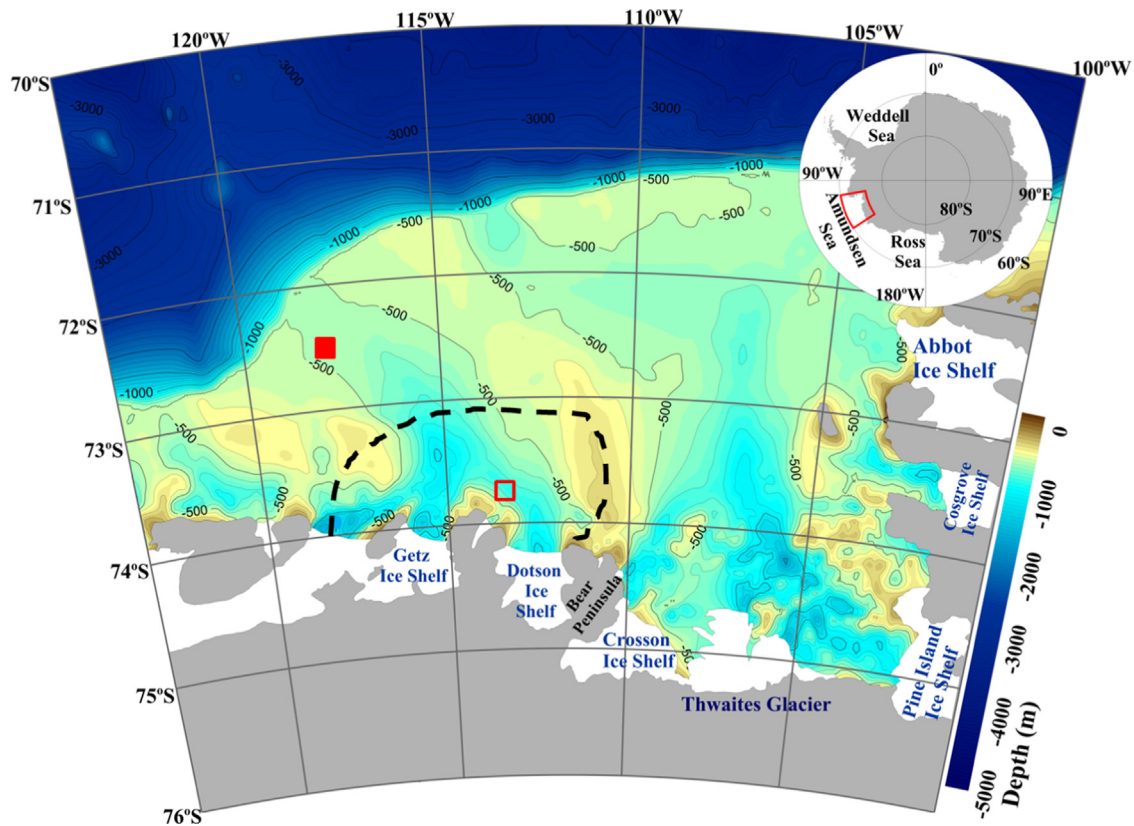


Fig. 1. Bathymetry of the study region. Sampling sites of sinking particles are also indicated (K1 trap in the SIZ=closed symbol, the US ASPIRE trap=open symbol). The dashed line indicates the 10% sea ice concentration in January 2011 as the boundary of the Amundsen Sea polynya.

The resultant CO_2 was cryogenically purified and stored in a Pyrex tube. The resultant CO_2 samples were analyzed for radiocarbon and stable carbon isotopes at the National Ocean Sciences Accelerator Mass Spectrometry Facility at Woods Hole Oceanographic Institution (NOSAMS WHOI) following standard techniques (McNichol et al., 1994). The uncertainty for this type of sample determined by multiple duplicate-analyses in our lab is less than 10‰ for $\Delta^{14}\text{C}$ (a fractionation-corrected value of $^{14}\text{C}/^{12}\text{C}$ relative to a standard (Broecker and Olson, 1959; Stuiver and Polach, 1977)) and 0.1‰ for $\delta^{13}\text{C}$. A subset of samples was analyzed for $\delta^{15}\text{N}$ values at KOPRI, using an elemental analyzer (Flash HT 2000) aligned with an isotope ratio mass spectrometer (Delta V plus).

One aliquot of each sample was examined under a dissecting microscope with dark field illumination (Olympus SZX16) at KOPRI for fecal pellets, *P. antarctica* colonies, and intact zooplankton. Although large and conspicuous swimmers had been removed, small and intact copepodites and zooplankton larva were observed. These undecomposed zooplankton were counted. Fecal pellets were examined using an inverted microscope (Olympus IX 70). Samples too dense for microscopic analysis were diluted until individual pellets were readily visible, and a 2–5 ml aliquot was pipetted into a petri dish with a grid.

3. Results

3.1. Particle flux

Total particle flux ranged between 4 and $780 \text{ mg m}^{-2} \text{ d}^{-1}$ (Table 1, Fig. 2a). The particle flux was greater than $200 \text{ mg m}^{-2} \text{ d}^{-1}$ at the beginning of the sampling period in January. The highest value, $780 \text{ mg m}^{-2} \text{ d}^{-1}$, was observed in mid-January 2011. A particle flux greater than $100 \text{ mg m}^{-2} \text{ d}^{-1}$ was maintained until mid-March,

and values of $\sim 30 \text{ mg m}^{-2} \text{ d}^{-1}$ were observed for the two following samples in March and April. From May 2011 to early January 2012, the particle flux remained below $15 \text{ mg m}^{-2} \text{ d}^{-1}$. The lowest flux was observed between June and October ($5.8 \text{ mg m}^{-2} \text{ d}^{-1}$ on average). The flux was slightly elevated in November but low again in early to mid-December, then was elevated for the remainder of the sampling period. Total annual particle flux was $28.6 \text{ g m}^{-2} \text{ yr}^{-1}$ (equivalent to an average daily flux of $78.2 \text{ mg m}^{-2} \text{ d}^{-1}$). Total particle flux during the austral summer (70 days for the first seven samples from January to mid-March) accounted for 87% of the annual flux.

Total particle flux appears to be coupled with the sea ice concentration at the surface. The sea ice concentration started to decrease at the beginning of December in 2010 and reached the minimum value, $\sim 37\%$, in early January (Fig. 2a). Unfortunately, our sampling started in January, and hence no particle flux data are available in December when the sea ice concentration decreased rapidly. The period of high particle flux lasted for at least 2 months, suggesting a prolonged bloom export. The abrupt decrease in total particle flux by mid-March was coincident with the recovery of sea ice to 85–100%. The depletion of micro- and/or macronutrients may have caused the observed decrease in particle flux, although no supporting data are available. Unlike the austral summer in 2010/2011, the sea ice concentration started to decrease much later in late January 2012, and the minimum value was $\sim 50\%$ in February 2012 at the mooring site. Therefore, our sample collection ended before sea ice melting began at the site. This distinct development in sea ice concentration appears to be correlated with the total particle flux registered by the trap during November and December 2011.

During the high particle flux period, from January to March 2011, the biogenic components accounted for 85% of the particle flux on average and were mainly represented by opal and organic matter. Opal flux ranged from 1 to $484 \text{ mg m}^{-2} \text{ d}^{-1}$ and accounted

Table 1

Sampling time, cup open interval, total particle and POC fluxes, contents of biogenic and non-biogenic components, molecular ratios, and carbon and nitrogen isotope values of sinking particles. Values in parenthesis are the contents of POM, opal, and CaCO₃ estimated from the elemental values. Note that each pair of samples, #13 and #14, #15 and #16, #17 and #18, and #20 and #21, was combined for isotopic analyses.

Cup #	Cup opening date (mm/dd/yy)	Sampling interval (days)	Total mass flux (mg m ⁻² d ⁻¹)	POC flux (mgC m ⁻² d ⁻¹)	POC (POM)%	Bio-Si (Opal)%	PIC (CaCO ₃)%	Non-biogenic (%) ^a	C/N ratio	Bio-Si/PIC ratio	Δ ¹⁴ C (‰)	δ ¹³ C (‰)	δ ¹⁵ N (‰) ^b	<i>P. antarctica</i> colony (No. m ⁻² d ⁻¹)	Fecal pellet (No. m ⁻² d ⁻¹)	Zoo plankton ^c (No./bottle)
1	1/5/11–1/14/11	9	255	22	8.7 (22)	24 (57)	0.1 (0.9)	20 ± 9	8.3	98	–176	–27.9	1.8	1E+2	4.2E+4	40
2	1/14/11–1/23/11	9	779	55	7.0 (18)	26 (62)	0.03 (0.3)	20 ± 9	8.6	340	–170	–27.4	1.6	8E+2	2.5E+5	ND ^d
3	1/23/11–2/1/11	9	511	33	6.5 (16)	31 (75)	0.1 (0.7)	8.1 ± 11	8.3	171	–169	–27.3	2.3	9E+2	1.7E+5	10
4	2/1/11–2/10/11	9	430	30	7.0 (17)	29 (69)	0.1 (0.9)	13 ± 10	8.2	118	–160	–27.2	3.0	8E+2	1.3E+5	ND
5	2/10/11–2/19/11	9	213	18	8.2 (21)	29 (69)	0.2 (1.5)	9.4 ± 10	8.1	70	–164	–27.1	3.4	1E+2	6.4E+4	10
6	2/19/11–3/1/11	10	361	19	5.2 (13)	28 (67)	0.1 (0.7)	19 ± 10	6.8	138	–174	–26.1	2.4	2E+2	6.9E+4	20
7	3/1/11–3/16/11	15	106	6.1	5.8 (14)	31 (74)	0.1 (1.0)	11 ± 11	6.9	109	–180	–26.3	3.1	5E+1	4.0E+4	10
8	3/16/11–4/1/11	16	34	3.3	9.7 (24)	25 (60)	0.2 (1.8)	14 ± 9	7.0	50	–184	–26.7	4.1	1E+1	1.0E+4	80
9	4/1/11–5/1/11	30	34	3.8	11 (28)	21 (49)	0.2 (1.9)	21 ± 7	7.0	39	–176	–27.2	5.2	ND	4E+3	90
10	5/1/11–6/1/11	31	12	1.9	16 (41)	15 (36)	0.6 (5.2)	18 ± 6	7.3	10	–169	–27.3	7.5	ND	8E+2	60
11	6/1/11–7/1/11	30	4	1.3	33 (83)	ND	1.0 (8.0)	ND	6.6	ND	ND	ND	ND	ND	6E+2	120
12	7/1/11–8/1/11	31	5	1.6	30 (75)	ND	0.6 (4.9)	ND	6.5	ND	–154	–27.9	ND	ND	2E+2	190
13	8/1/11–9/1/11	31	6	1.2	21 (52)	11 (27)	1.2 (9.7)	11 ± 4	6.9	4.1	–172	–27.1	ND	ND	2E+2	140
14	9/1/11–10/1/11	30	7	1.8	24 (60)	6 (14)	1.0 (8.0)	18 ± 2	6.8	2.5			ND	ND	2E+2	180
15	10/1/11–11/1/11	31	7	1.2	16 (41)	7 (17)	1.1 (8.8)	34 ± 3	6.6	2.8	–215	–26.8	ND	ND	2E+2	20
16	11/1/11–11/16/11	15	15	1.5	10 (24)	9 (21)	1.2 (9.6)	45 ± 3	7.2	3.2			ND	ND	4E+2	30
17	11/16/11–12/1/11	15	14	1.3	8.8 (22)	6 (15)	1.4 (12)	51 ± 2	7.3	1.8	–232	–27.2	ND	ND	3E+2	20
18	12/1/11–12/10/11	9	5	ND	ND	ND	1.8 (15)	ND	ND	ND			ND	ND	2E+2	ND
19	12/10/11–12/19/11	9	10	ND	ND	ND	1.5 (12)	ND	ND	ND	ND	ND	ND	ND	2E+2	ND
20	12/19/11–12/28/11	9	13	1.5	11 (28)	ND	1.8 (15)	ND	6.9	ND	–252	–26.1	ND	ND	2E+2	20
21	12/28/11–1/5/12	8	14	1.1	7.8 (19)	ND	1.3 (11)	ND	7.6	ND			ND	ND	6E+2	10
Annual flux			29 g yr ⁻¹	2.2 gC yr ⁻¹												

^a The uncertainty is a propagated error.

^b Measurements on total nitrogen.

^c Zooplankton implies small intact zooplankton, including copepodites and larva, observed under the microscope after the initial removal of swimmers.

^d ND=No data.

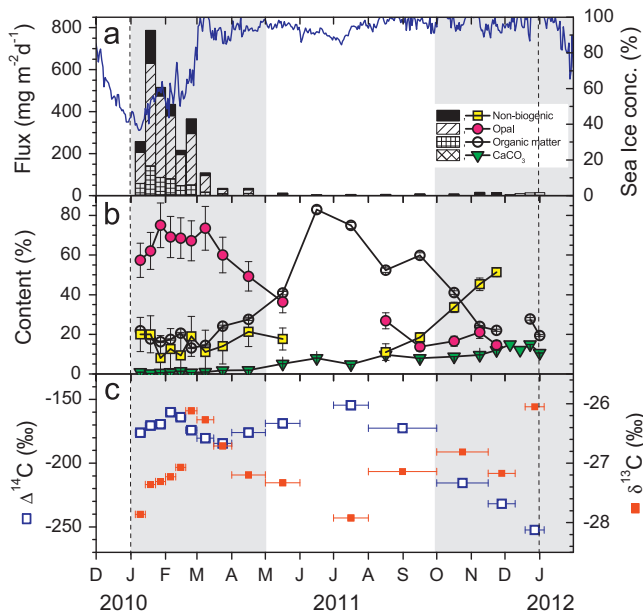


Fig. 2. (a) Fluxes of non-biogenic particles, opal, organic matter, and CaCO_3 (left y-axis) and sea ice concentration in the surface (right y-axis) at the sampling site; (b) relative contents (%) of biogenic and non-biogenic components in sinking particles (square=non-biogenic, closed circle=opal, open circle=organic matter, reversed triangle= CaCO_3); and (c) carbon isotope values of sinking POC (open square= $\Delta^{14}\text{C}$, closed square= $\delta^{13}\text{C}$). Horizontal error bars denote the periods that each sample represents. The shades indicate periods divided for discussion (see text).

for the major portion of sinking particle flux during this period. Highest opal fluxes were registered in January and February (up to $146 \text{ mg m}^{-2} \text{ d}^{-1}$). From March, the opal flux started to decrease gradually until lower than $4 \text{ mg m}^{-2} \text{ d}^{-1}$ in May. CaCO_3 flux was extremely low ($< 4 \text{ mg m}^{-2} \text{ d}^{-1}$) compared with the other biogenic components throughout the study period. The CaCO_3 flux was several-fold higher from January to mid-March than that during the austral winter. The peak CaCO_3 flux was observed in early February, unlike total particle flux or opal flux, which peaked in mid-January. CaCO_3 flux was elevated two- to three-fold from November 2011 to the end of the sample collection.

Seasonal variation of the POC flux was similar to that of the total particle flux (Figs. 2a and 4). Annual average POC flux (sampling duration-weighted) was $6 \text{ mgC m}^{-2} \text{ d}^{-1}$ and total annual flux was $2.2 \text{ gC m}^{-2} \text{ yr}^{-1}$. POC flux during the austral summer from January to mid-March accounted for 77% of the total annual flux.

The flux of non-biogenic components ranged between 1 and $156 \text{ mg m}^{-2} \text{ d}^{-1}$ when estimates were available. The flux was greater than $20 \text{ mg m}^{-2} \text{ d}^{-1}$ in January and February 2011. After March, the flux decreased to $1 \text{ mg m}^{-2} \text{ d}^{-1}$ and remained low during the austral winter. The non-biogenic particle flux started to increase again in October.

3.2. Particle composition

Contents (%) of each biogenic component and non-biogenic components show a different seasonal variation from that of the flux (Fig. 2b). During the high-flux period from January to March 2011, opal accounted for 67% of total particle flux on average (Fig. 2b). The remainder was accounted for almost equally by organic matter and non-biogenic components. The contribution of opal to total particle flux was dominant until the end of April and decreased gradually until accounting for 10–20% of the particles (note the lack of data for June, July, and December because of

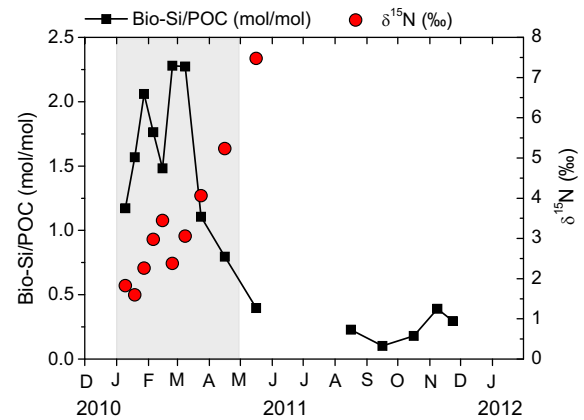


Fig. 3. Bio-Si/POC molar ratio (square; left y-axis) and $\delta^{15}\text{N}$ (‰) values (circle; right y-axis) for available samples. The shaded area indicates the period of high particle flux (see text).

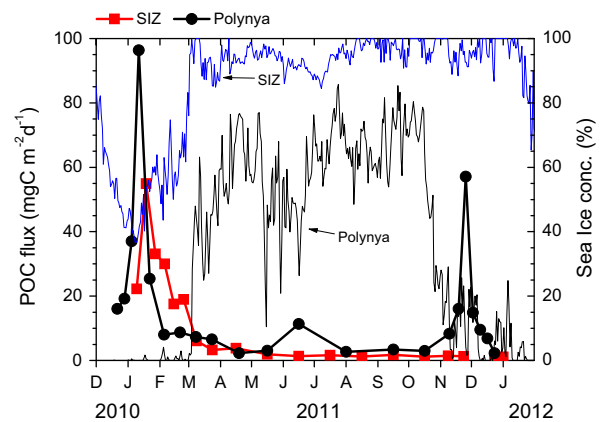


Fig. 4. POC flux and sea ice concentration at the K1 site in the SIZ (squares) and at the US ASPIRE site inside the Amundsen Sea polynya (circles, Ducklow et al. (2015)).

insufficient sample amounts). In contrast, organic matter accounted for $\sim 19\%$ during the high-flux period and then became the dominant contributor from May to October (41–83%). During June and July, when total particle fluxes reach the annual minimum, the contribution of organic matter was the highest on record, over 75%. After December, the organic matter content decreased to values similar to those during the high-flux period. CaCO_3 accounted for the smallest fraction of the sinking particles. CaCO_3 content was less than 1% during the high-flux period and increased gradually up to 15% in December. The non-biogenic components accounted for 10–20% until September, then its contribution increased gradually in October and November, reaching $\sim 50\%$. The non-biogenic components were likely to account for a high value in December as well, although the value was not estimated because of a lack of opal content data. However, if the flux was considered, non-biogenic material flux was ~ 10 fold higher in January and February ($65 \text{ mg m}^{-2} \text{ d}^{-1}$) than in October and November ($6 \text{ mg m}^{-2} \text{ d}^{-1}$).

The C/N molar ratio varied between 6.5 and 8.6 (Table 1). The value was over 8 for the first five samples in January and early February. From mid-February, the ratio decreased to below 7 and remained low. The lowest values were observed in June and July. The Bio-Si/PIC molar ratio ranged from 2 to 340. The ratios were comparatively high in January, February, and early March (higher than 70) and decreased rapidly to a value of 2 in late December.

The number of fecal pellets ranged from 200 to 250,000, temporally covarying with total particle flux (Table 1). The number of *P. antarctica* colonies also showed a similar temporal variation

with total particle flux. However, the number of small and intact zooplankton, including copepodites and larva, was low during the period of high particle flux in January and February, but distinctly higher between March and September, and then low again from October to December.

3.3. Isotopic compositions

$\Delta^{14}\text{C}$ values of sinking POC ranged between -252‰ and -154‰ (Fig. 2c). The $\Delta^{14}\text{C}$ value increased from -176‰ to -160‰ then decreased to -184‰ during the high-flux period; it increased to -154‰ in July and decreased to -252‰ in December. Low values were observed in October through December 2011 ($-233 \pm 19\text{‰}$ on average). Except for these low values, the observed values were within the range of those of suspended POC collected in the surface water on the Amundsen Shelf during the expedition in February and March 2012 when the sediment trap was recovered ($-149 \pm 26\text{‰}$, $n=5$; Kim et al., submitted).

$\delta^{13}\text{C}$ values of sinking POC ranged between -27.9 and -26.1‰ . The $\delta^{13}\text{C}$ values increased in January and February, then decreased from the highest value in March to the lowest in July. The temporal variation in $\delta^{13}\text{C}$ mirrored that of $\Delta^{14}\text{C}$ from April to the end of the sample collection.

$\delta^{15}\text{N}$ values of sinking POM ranged between 1.6 and 7.5‰ for the first 10 samples (Table 1, Fig. 3). The $\delta^{15}\text{N}$ values increased from low values seen in January until May. The average $\delta^{15}\text{N}$ value in April and May (6.4‰) was considerably higher than that during the high particle flux period (2.7‰).

4. Discussion

4.1. Seasonal variation in particle source

In this section, considering the physical environment such as sea ice concentration and solar irradiation, and the observed particle composition and radiocarbon content, we discuss the sources of sinking particles during three time periods: (i) from January to April when primary production was active, sea ice concentration low, and sinking particle flux high; (ii) from May to September when photosynthetically active radiation was negligible, sea ice concentration > 90%, and particle flux extremely low; and (iii) from October to mid-January when the contribution of non-biogenic components was high. These three periods roughly correspond to austral summer, winter, and spring, respectively.

During the first period of the austral summer, opal was dominant in sinking particles. This is consistent with observations in late December 2010 and January 2011, during which diatoms were dominant among the phytoplankton community in surface waters in the SIZ (Lee et al., 2012). Diatoms reportedly account for > 90% of the carbon biomass in the surface water at the mooring site (Lee et al., 2012). In addition to diatoms, a large number of *P. antarctica* colonies was observed in the sinking particle samples.

During the second period, opal decreases in both flux and content and a coincident increase in organic matter content from March to May imply that the diatom-dominated phytoplankton community shifted toward other dominant organisms such as zooplankton. POC content was extremely high, over 30% equivalent to over 70% as organic matter, in June and July, although the total particle flux was very low (Fig. 2b). *P. antarctica* colonies were not observed under the microscope in the samples from April (Table 1). Instead, intact bodies of copepods and nauplii were found abundantly in the sinking particle samples during this period. These intact zooplankton may be a part of the vertically migrating organisms (La et al., 2015). The zooplankton may feed on the actively growing sea ice algae in austral fall (Fritsen et al.,

1994). Another possibility is that the copepods growing in sea ice during late austral summer (Schnack-Schiel et al., 1998) may have been released from the ice during austral fall and winter. A good positive correlation between POC% and $\delta^{15}\text{N}$ ($R^2=0.8$) further supports the high contribution of zooplankton. $\delta^{15}\text{N}$ values in April and May were higher than those in January and February by $\sim 4\text{‰}$, corresponding to one trophic level increase (Peterson and Fry, 1987), if this was indeed caused by an increase in trophic level (Fig. 3). The Bio-Si/POC molar ratio was higher than 1 until March and was lower than 0.5 for the rest of the time period with available data, clearly demonstrating a shift in the dominant particle source (Fig. 3).

During the third period, POC% decreased from 24% in September to $\sim 10\%$ in November. CaCO_3 flux and opal flux doubled during the first half of November, caused mainly by pteropods and radiolarian species, respectively, implying that biological production in the surface water started to increase. The supply of ice algae or organic matter released by ice melting may be excluded as a potential source of the enhanced flux of CaCO_3 and opal, because the sea ice concentration did not change in November or December. However, the particle samples were not examined for the existence of ice algae to support this. The $\Delta^{14}\text{C}$ value of organic matter derived from sediment would be considerably lower than that derived from phytoplankton in the surface water. Low $\Delta^{14}\text{C}$ values toward the end of the sampling period, from October 2011 to early January 2012, are probably related to resuspended sediment and/or particles entrained in the glacier and released to sea water by glacial melting. The content of the non-biogenic particles showed a negative correlation with the $\Delta^{14}\text{C}$ value of sinking POC ($R^2=0.82$), supporting the concept that the non-biogenic particles are likely derived from aged source(s).

Considering the proximity of the trap to the seafloor and the topographic setting of the mooring site on the slope of the Dotson Trough, we suspected that sediment resuspension, and hence the non-biogenic components, may account for a considerable portion of the sinking material as observed in the Ross Sea (Dunbar et al., 1998). However, the $\Delta^{14}\text{C}$ values of sinking POC from January 2011 to September 2011 were within the range of those of the suspended POC in the surface waters on the Amundsen Shelf (Kim et al., submitted). The suspended POC in the surface water was likely a mixture of POC from various sources, such as that released from melting sea ice and icebergs, detached land-fast ice, and eolian input. The rather large variation in $\Delta^{14}\text{C}$ of the suspended POC in surface waters ($-149 \pm 26\text{‰}$, $n=5$; Kim et al., submitted) may be evidence for various sources of suspended POC. However, the average $\Delta^{14}\text{C}$ value of the suspended POC was virtually identical to that of dissolved inorganic carbon in the surface water at the mooring station (-153‰ ; M. Kim and J. Hwang, unpublished data, 2014) within analytical uncertainty. Therefore, in general, sinking POC, except for the samples collected in October through December, is considered to originate mainly from fresh biological production in the surface water (however, note that radiocarbon cannot be used to differentiate the resuspension of unconsolidated, relatively fresh organic matter because of its long half-life, 5730 years). In terms of particle flux, the contribution of non-biogenic components was the highest during the first period when particle flux was highest. This result may be related to the current speed, which was higher during this period ($7.5 \pm 3.3 \text{ cm s}^{-1}$ on average) than the other months ($4.4 \pm 2.4 \text{ cm s}^{-1}$). Other than this, no obvious correlation was observed between the contribution of non-biogenic particles and the current speed.

4.2. Spatial variation of POC flux

We compared our sinking POC flux data with those obtained inside the Amundsen Sea polynya by the US ASPIRE during the same period (Fig. 4). At this site, the sea ice concentration

decreased to nearly nonexistent levels in November 2010, and the ice-free condition was maintained for over 3 months from mid-November to the end of February (Ducklow et al., 2015). The ice concentration afterward fluctuated between ~30% and 90%. The highest POC flux was observed in early January when an intense but short-lived pulse of enhanced POC export (up to $96 \text{ mgC m}^{-2} \text{ d}^{-1}$), apparently due to a phytoplankton bloom, was registered by the trap (Ducklow et al., 2015). The peak flux of sinking POC inside the polynya was about twice that in the SIZ. However, comparison of the time-integrated POC fluxes during the austral summer yields an interesting point. High POC flux lasted longer in the SIZ: the POC flux in the SIZ was approximately twice that inside the polynya in February. Consequently, the POC fluxes integrated over the austral summer were virtually identical between the two sites (the POC fluxes integrated over January and February were 1.6 and 1.3 gC m^{-2} in the SIZ and inside the polynya, respectively). There is a concern that this result may in part have been caused by different trapping efficiencies between two types of sediment traps considering the current speed up to 17 cm s^{-1} observed at our site (Buesseler et al., 2010). This possibility is discussed in detail in Ducklow et al. (2015). Also, it cannot be ruled out that this disparity may have been caused by inclusion of resuspended, unconsolidated fresh organic matter from the water-sediment boundary, considering the height of the sediment traps from the sea floor (130 m versus 450 m, in the SIZ and inside the polynya, respectively).

These results may have an important implication for the estimation of sinking POC flux on the Amundsen Shelf based on the primary production data. Primary productivity determined by the *in situ* ^{13}C incorporation rate was considerably different between inside the Amundsen Sea polynya and the SIZ (Lee et al., 2012). The average daily carbon production rate of phytoplankton observed from December 21, 2010 to January 23, 2011 was $2.2 \pm 1.4 \text{ gC m}^{-2} \text{ d}^{-1}$ inside the Amundsen Sea polynya versus $0.2 \pm 0.3 \text{ gC m}^{-2} \text{ d}^{-1}$ in non-polynya areas of the Amundsen Sea (Lee et al., 2012). The POC fluxes in the austral summer at the two sites were not commensurate with primary productivity in the surface waters.

Very different export efficiencies may be conjectured based on similar time-integrated POC fluxes, despite the largely different primary productivities between the two locations. Ducklow et al. (2015) estimated the annual POC flux over annual primary production inside the polynya to be ~5% based on the satellite-based data and their sediment trap study. A similarly low ratio (~1%) was observed at 200 m in the Ross Sea (Smith and Gordon, 1997; Collier et al., 2000). Unfortunately, no satellite observation is available at our SIZ site for this kind of estimation. The *f*-ratios (export production) estimated from the *in situ* determination of nitrate and ammonium uptake rates were higher in the SIZ (0.76 ± 0.16) than in the polynya (0.60 ± 0.09) (Lee et al., 2012), although the difference in the *f*-ratios may not be large enough to fully account for the disparity in export flux at the two sites. A potential reason for this difference in *f*-ratio and presumed difference in the export efficiency may be the distinct composition of the phytoplankton community. During the campaign in 2010/2011, the trap mooring site in the SIZ was almost exclusively inhabited by diatoms in terms of carbon biomass (Lee et al., 2012), which is consistent with the dominance of opal in the particle flux during the high-flux period. In contrast, inside the polynya, *P. antarctica* and diatoms contributed almost equally to the phytoplankton community (Lee et al., 2012). Diatoms are likely to be more prone to vertical export than are *P. antarctica* (Reigstad and Wassmann, 2007).

If the observed relationship between primary production and POC flux can be extrapolated to the wider regions of the Amundsen Shelf where the sea ice concentration and phytoplankton community in summer were similar to those at our site, sinking POC flux to the interior water column may be considerably higher than previously thought. Whether the phenomenon we observed

is a general feature, regarding the polynyas and SIZ, needs to be examined more carefully by extending the spatial and temporal coverage of the observation.

5. Summary and conclusions

We have examined sinking particle flux at a depth of 400 m using a time-series sediment trap deployed in the SIZ on the Amundsen Shelf. The biological carbon pump beyond primary production in the surface water has not been examined in this region. We focused on characterization of the sinking particle flux in the SIZ and compared our data with those obtained from inside the Amundsen Sea polynya by the US ASPIRE to gain insights on the spatial variability in sinking POC flux.

The major portion of sinking particle flux occurred during the austral summer. Consistent with the diatom-dominated phytoplankton community in the corresponding surface water, particle flux was dominated by opal flux during this high-flux period. This opal dominance was replaced by POM from June to September potentially supported by zooplankton. $\Delta^{14}\text{C}$ values of the winter samples indicated a sustained supply of fresh POM to the water column. Contribution by zooplankton in the winter may be indicated by the increase in the $\delta^{15}\text{N}$ value by approximately 4‰ from the austral summer to winter values. Contribution from sediment resuspension to sinking particles was small considering the low content of non-biogenic components. One exception was observed from October to December, when $\Delta^{14}\text{C}$ values were lower than the annual average, and non-biogenic components accounted for over 30% of the sinking particles.

An interesting observation was that the sinking POC flux integrated over the austral summer in the SIZ was comparable to that inside the Amundsen Sea polynya, although the maximum POC flux and primary productivity determined *in situ* were significantly higher inside the polynya. These results are thought to be caused by longer lasting primary production (hence POC flux) and higher export efficiency, potentially owing to the diatom-dominated plankton community in the SIZ compared with inside the polynya. This observation may hold an important implication when one attempts to estimate the shelf-wide POC flux. This aspect warrants further investigation by expanding the spatial and temporal coverage of research on the Amundsen Shelf.

Acknowledgements

We thank the captain and crew of the IBRV *Araon* for help at sea, Ho kyung Ha and Tae Wan Kim for current meter data, NOSAMS WHOI for carbon isotopic analyses, Haryun Kim, Borom Lee, and Seung-II Nam for $\delta^{15}\text{N}$ analysis, HuiTae Joo and Bo Kyung Kim for *in situ* primary production data, and all cruise participants for their help. This research was supported by the Korea Polar Research Institute (PP14020).

References

- Alderkamp, A.-C., Mills, M.M., van Dijken, G.L., Laan, P., Thuróczy, C.-E., Gerringa, L. J., de Baar, H.J., Payne, C.D., Visser, R.J., Buma, A.G., 2012. Iron from melting glaciers fuels phytoplankton blooms in the Amundsen Sea (Southern Ocean): phytoplankton characteristics and productivity. *Deep-Sea Res. II* 71, 32–48.
- Arrigo, K.R., Robinson, D.H., Worthen, D.L., Dunbar, R.B., DiTullio, G.R., VanWoert, M., Lizotte, M.P., 1999. Phytoplankton community structure and the drawdown of nutrients and CO_2 in the Southern Ocean. *Science* 283, 365–367.
- Arrigo, K.R., van Dijken, G.L., 2003. Phytoplankton dynamics within 37 Antarctic coastal polynya systems. *J. Geophys. Res.* 108, 3271.
- Arrigo, K.R., van Dijken, G.L., Bushinsky, S., 2008. Primary production in the Southern Ocean, 1997–2006. *J. Geophys. Res.* 113, C08003.

- Arrigo, K.R., Lowry, K.E., van Dijken, G.L., 2012a. Annual changes in sea ice and phytoplankton in polynyas of the Amundsen Sea, Antarctica. *Deep-Sea Res. II* 71–76, 5–15.
- Arrigo, K.R., Perovich, D.K., Pickart, R.S., Brown, Z.W., van Dijken, G.L., Lowry, K.E., Mills, M.M., Palmer, M.A., Balch, W.M., Bahr, F., 2012b. Massive phytoplankton blooms under Arctic sea ice. *Science* 336, 1408.
- Broecker, W.S., Olson, E.A., 1959. Lamont radiocarbon measurements VI. *Am. J. Sci.* 1, 111–132.
- Buesseler, K.O., McDonnell, A.M., Schofield, O.M., Steinberg, D.K., Ducklow, H.W., 2010. High particle export over the continental shelf of the west Antarctic Peninsula. *Geophys. Res. Lett.* 37, L22606.
- Collier, R., Dymond, J., Honjo, S., Manganini, S., Francois, R., Dunbar, R., 2000. The vertical flux of biogenic and lithogenic material in the Ross Sea: moored sediment trap observations 1996–1998. *Deep-Sea Res. II* 47, 3491–3520.
- DeMaster, D.J., 1981. The supply and accumulation of silica in the marine environment. *Geochim. Cosmochim. Acta* 45, 1715–1732.
- DiTullio, G., Grebmeier, J., Arrigo, K., Lizotte, M., Robinson, D., Leventer, A., Barry, J., VanWoert, M., Dunbar, R., 2000. Rapid and early export of *Phaeocystis antarctica* blooms in the Ross Sea, Antarctica. *Nature* 404, 595–598.
- Ducklow, H.W., Erickson, M., Lee, S., Lowry, K., Post, A., Sherrell, R., Stammerjohn, S., Wilson, S., Yager, P., 2015. Particle flux on the continental shelf in the Amundsen Sea Polynya and Western Antarctic Peninsula. *Elementa* 3, 000046.
- Dunbar, R.B., Leventer, A.R., Mucciarone, D.A., 1998. Water column sediment fluxes in the Ross Sea, Antarctica: atmospheric and sea ice forcing. *J. Geophys. Res.* 103, 30741–30759.
- Fritsen, C., Lytle, V., Ackley, S., Sullivan, C., 1994. Autumn bloom of Antarctic pack-ice algae. *Science* 266, 782–784.
- Ha, H., Wählin, A., Kim, T., Lee, S., Lee, J., Lee, H., Hong, C., Arneborg, L., Björk, G., Kalén, O., 2014. Circulation and modification of warm deep water on the central Amundsen Shelf. *J. Phys. Oceanogr.* 44, 1493–1501.
- Hedges, J.L., Stern, J.H., 1984. Carbon and nitrogen determinations of carbonate-containing solids. *Limnol. Oceanogr.* 29, 657–663.
- Kim, H.J., Hyeong, K., Yoo, C.M., Khim, B.K., Kim, K.H., Son, J.W., Kug, J.S., Park, J.Y., Kim, D., 2012. Impact of strong El Niño events (1997/98 and 2009/10) on sinking particle fluxes in the 10°N thermocline ridge area of the northeastern equatorial Pacific. *Deep-Sea Res. I* 67, 111–120.
- Kim, M., Hwang, J., Lee, S.H., Kim, H.J., Kim, D., Lee, S., Submitted. Characteristics of sedimentation of particulate organic carbon on the Amundsen Shelf, Antarctica. *Deep-Sea Res. II*.
- Komada, T., Anderson, M.R., Dorfmeier, C.L., 2008. Carbonate removal from coastal sediments for the determination of organic carbon and its isotopic signatures, $\delta^{13}\text{C}$ and $\Delta^{14}\text{C}$: comparison of fumigation and direct acidification by hydrochloric acid. *Limnol. Oceanogr. Methods* 6, 254–262.
- La, H.S., Ha, H.K., Kang, C.Y., Wählin, A.K., Shin, H.C., 2015. Acoustic backscatter observations with implications for seasonal and vertical migrations of zooplankton and nekton in the Amundsen, Shelf (Antarctica). *Estuarine Coastal Shelf Sci.* 152, 124–133.
- Lee, S.H., Kim, B.K., Yun, M.S., Joo, H., Yang, E.J., Kim, Y.N., Shin, H.C., Lee, S., 2012. Spatial distribution of phytoplankton productivity in the Amundsen Sea, Antarctica. *Polar Biol.* 35, 1721–1733.
- Lizotte, M.P., 2001. The contributions of sea ice algae to Antarctic marine primary production. *Am. Zool.* 41, 57–73.
- McNichol, A., Osborne, E., Gagnon, A., Fry, B., Jones, G., 1994. TIC, TOC, DIC, DOC, PIC, POC—unique aspects in the preparation of oceanographic samples for 14C-AMS. *Nucl. Instrum. Methods Phys. Res., Sect. B: Beam Interact. Mater. At.* 92, 162–165.
- Mortlock, R.A., Froelich, P.N., 1989. A simple method for the rapid determination of biogenic opal in pelagic marine sediments. *Deep-Sea Res. I* 36, 1415–1426.
- Otosaka, S., Tanaka, T., Togawa, O., Amano, H., Karasev, E.V., Minakawa, M., Noriki, S., 2008. Deep sea circulation of particulate organic carbon in the Japan Sea. *J. Oceanogr.* 64, 911–923.
- Peterson, B.J., Fry, B., 1987. Stable isotopes in ecosystem studies. *Annu. Rev. Ecol. Syst.* 18, 293–320.
- Reigstad, M., Wassmann, P., 2007. Does *Phaeocystis* spp. contribute significantly to vertical export of organic carbon? *Biogeochemistry* 83, 217–234.
- Schnack-Schiel, S.B., Thomas, D.B., Dahms, H.-U., Hass, C.B., Mizdalski, E.B., 1998. Copepods in Antarctic sea ice. *Antarct. Res. Ser.* 73, 173–182.
- Smith Jr, W.O., Gordon, L.L., 1997. Hyperproductivity of the Ross Sea (Antarctica) polynya during austral spring. *Geophys. Res. Lett.* 24, 233–236.
- Smith Jr, W.O., Ainley, D.G., Arrigo, K.R., Dinniman, M.S., 2014. The oceanography and ecology of the Ross Sea. *Ann. Rev. Mar. Sci.* 6, 469–487.
- Stammerjohn, S., Massom, R., Rind, D., Martinson, D., 2012. Regions of rapid sea ice change: an inter-hemispheric seasonal comparison. *Geophys. Res. Lett.* 39, L0501.
- Stuiver, M., Polach, H.A., 1977. Discussion; reporting of C-14 data. *Radiocarbon* 19, 355–363.
- Thomas, D.N., Lara, R.J., Haas, C.J., Schnack-Schiel, S.B., Dieckmann, G.S., Kattner, G., Nöthig, E., Mizdalski, E.S., 1998. Biological soup within decaying slimmer sea ice in the Amundsen Sea, Antarctica. *Antarct. Res. Ser.* 73, 161–171.
- Thomas, D.N., Dieckmann, G.S., 2002. Antarctic sea ice—a habitat for extremophiles. *Science* 295, 641–644.
- Thunell, R.C., 1998. Seasonal and annual variability in particle fluxes in the Gulf of California: a response to climate forcing. *Deep-Sea Res. I* 45, 2059–2083.
- Wählin, A., Yuan, X., Björk, G., Nohr, C., 2010. Inflow of Warm Circumpolar Deep Water in the central Amundsen Shelf. *J. Phys. Oceanogr.* 40, 1427–1434.
- Walker, D.P., Brandon, M.A., Jenkins, A., Allen, J.T., Dowdeswell, J.A., Evans, J., 2007. Oceanic heat transport onto the Amundsen Sea shelf through a submarine glacial trough. *Geophys. Res. Lett.* 34, 1–4.
- Yager, P., Sherrell, L., Stammerjohn, S., Alderkamp, A., Schofield, O., Abrahamsen, E., Arrigo, K., Bertilsson, S., Garay, D., Guerrero, R., 2012. ASPIRE: the Amundsen Sea Polynya International Research Expedition. *Oceanography* 25, 40–53.